



ROBOSAT Deliverable

D3.1 Intermediate report on GIS-based improvements of GNSS-based navigation for wild places and unconstrained environments

Yelyzaveta Pervysheva¹, Muhammad Safi¹, Elena Simona Lohan¹ and Andrei Cramariuc²

¹Tampere University

²AETH

Date March 28, 2026

Abstract

Reliable satellite navigation in wild and unconstrained environments remains challenging due to signal attenuation, multipath propagation, and rapidly changing environmental conditions. This deliverable presents the intermediate results within ROBOSAT project about how geographic information system (GIS) data could be used to enhance the performance, robustness, and interpretability of Global Navigation Satellite System (GNSS) positioning for robotic platforms operating outside structured urban infrastructure.

The proposed approach considers the integration of environmental context derived from open geospatial datasets, including digital elevation models, land-cover and vegetation layers, and vector representations of terrain features. These data sources are used to characterize propagation conditions, estimate line-of-sight availability, and support environment-aware filtering and weighting of GNSS observables. This deliverable discusses several integration strategies at different stages of the navigation pipeline, including pre-correlation domain, post-correlation domain, measurement-domain quality assessment, and post-processing fusion with trajectory estimation methods.

A preliminary system architecture is discussed for combining GNSS measurements, receiver-level quality indicators, and GIS-derived environmental descriptors within a unified processing framework suitable for robotic navigation. Particular attention is given to scalable processing workflows, the use of open data repositories, and compatibility with commonly used positioning tools and scientific computing environments.

The results highlight the potential of GIS-assisted navigation to improve positioning reliability in forests, mountainous terrain, and other environments where satellite visibility and signal quality are highly variable. The report outlines ongoing developments toward quantitative evaluation using ground-truth trajectories and multi-sensor robotic datasets.

Keywords: GNSS; GIS; robotic navigation; environmental context; multipath mitigation; terrain analysis

1. Robotic platform

At the Robotic Systems Lab (RSL) at ETH Zurich, we develop intelligent, legged robotic systems capable of operating in challenging and complex environments. ANYmal is a quadrupedal robot originally developed at our lab and now being produced by a large-scale (external to ROBOSAT) spinoff, ANYbotics AG. The robot is engineered for versatility to be able to walk, climb, and adapt to rugged terrain, making it an ideal commercial solution for industrial inspection, which is the main focus at ANYbotics. At RSL, though, we use the robotic platform to push the boundaries of research in control, perception, and autonomy. We are currently bringing the robot to more wild, uncontrolled outdoor environments and exploring the limits of its capabilities. As a legged platform ANYmal can traverse terrains and reach places that other robots are not able. In contrast to drones, the robot has a significantly larger payload (15kg) and can therefore function as a platform to deploy equipment and devices. The robot also carries a standard payload with multiple cameras and a 3D sensor (LiDAR) to enable autonomy and transmit data back to a remote operator. With our mounted sensor payload (detailed in D2.1) we significantly extend the perceptive capabilities of the robot and enable it to better function as a data-collection platform for

GIS data. Images of the robot in relevant environments and carrying the aforementioned custom sensor payload are shown in Figure 1.

2. GIS data repositories and show cases

Table 1 summarizes several national geospatial data repositories that provide datasets suitable for GNSS–GIS integration, environmental modelling, and robotics navigation studies.

All GIS layers shown in Fig. 2 were collected from the **Pirkkola region of Helsinki**, using openly available datasets provided by the National Land Survey of Finland NLS. The image was produced by the authors based on these data sources. The maps were processed and visualized in QGIS. In our planned implementation, route planning will guide the robot along predefined paths, while GNSS log files will be continuously monitored to assess localization performance and provide feedback for post-mission analysis.

2.0.1. Switzerland Showcase

To evaluate the integration of high-resolution GIS data with GNSS observations in complex terrain, a case study was conducted using datasets from Switzerland. The trajectory used in this experiment was extracted from the onboard navigation



Figure 1. Images of the ANYmal quadrupedal robot with our custom-designed sensor suite, detailed in D2.1, in various testing and recording environments.

Table 1. Examples of national GIS repositories relevant for GNSS and robotics research

Country	Repository (Link)	Main Data Available	Update Frequency
Finland	National Land Survey of Finland (NLS) maanmittauslaitos.fi	Topographic database, buildings, DEM, orthophotos, laser scanning, administrative boundaries	Continuously updated; orthophotos typically every 2–3 years
Switzerland	swisstopo swisstopo.admin.ch	High-resolution DEM, orthophotos, 3D buildings, national maps, geodetic reference data	Regular national updates
Romania	ANCPI Geoportal geoportal.ancpi.ro	Cadastral parcels, orthophotos, administrative boundaries, INSPIRE datasets	Periodic national updates
Spain	Instituto Geográfico Nacional (IGN) ign.es	Topographic maps, DEM, orthophotos, land cover, geodetic networks	Regular updates through national mapping programs

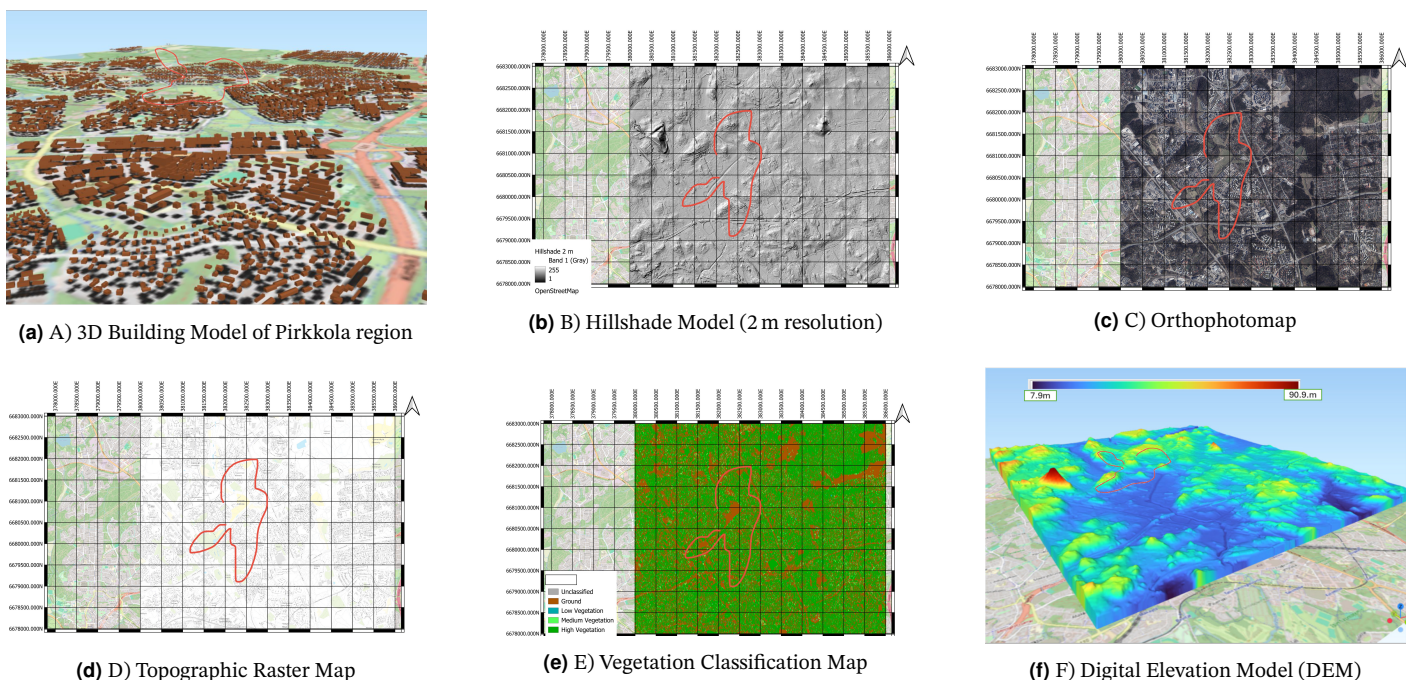


Figure 2. Visualisation of GIS layers used for autonomous robot navigation in the Pirkkola region of Helsinki. The red line illustrates the trajectory of the robot, as recorded, for example, with a GNSS app, such as GNSS Logger .

system of the ANYmal-D robotic platform equipped with a dual-antenna GNSS receiver (NovAtel CPT7). The receiver

logs provided time-synchronized positioning data, which were subsequently aligned and visualized together with geospatial

layers.

For environmental modelling, high-resolution geospatial products from the Swiss Federal Office of Topography (swisstopo) were used. These datasets are derived from airborne laser scanning and photogrammetric measurements and provide detailed classification of surface structures, including terrain, buildings, and vegetation canopy. Such classifications enable the identification of potential sources of signal obstruction, attenuation, and multipath, which are critical factors in GNSS positioning performance.

Two main geospatial layers were used:

- A Digital Elevation Model (DEM), representing the bare-earth surface and enabling terrain masking analysis and horizon estimation.
- Classified surface models derived from laser scanning, allowing discrimination between buildings, vegetation canopy, and open terrain, which are essential for line-of-sight (LOS) and non-line-of-sight (NLOS) assessment.

Figure 3 illustrates the high-resolution DEM used for terrain modelling, while Figure 4 presents a 3D visualization of classified surface data, where different surface types can be visually distinguished and the robot trajectory is overlaid. These layers provide complementary information: the DEM captures terrain morphology, whereas the classified surface model captures above-ground structures influencing GNSS signal propagation.

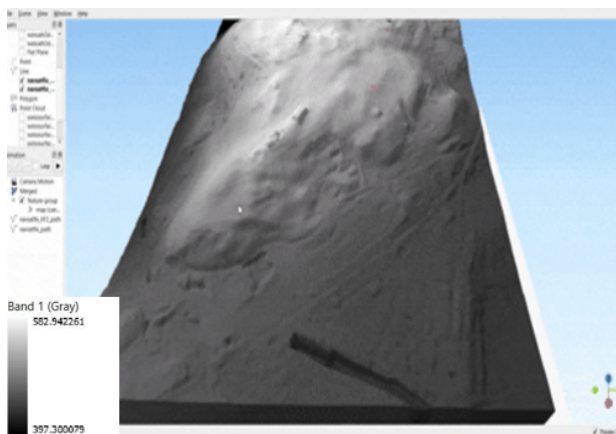


Figure 3. High-resolution digital elevation model (DEM) derived from airborne laser scanning, used for terrain modelling and masking analysis.

3. GIS -GNSS integration - preliminary architecture

The frontend is the part the operator or robot interacts with, showing the robot's status, maps, and mission planning tools, and allowing alerts to be set up. The backend handles the heavier tasks in the background, such as storing and processing GIS data, distributing GNSS corrections, and managing communication and alerts. **Roles:**

- *Operator* – configures the system if required; can also be automated.
- *User (Robot)* – autonomous robot;

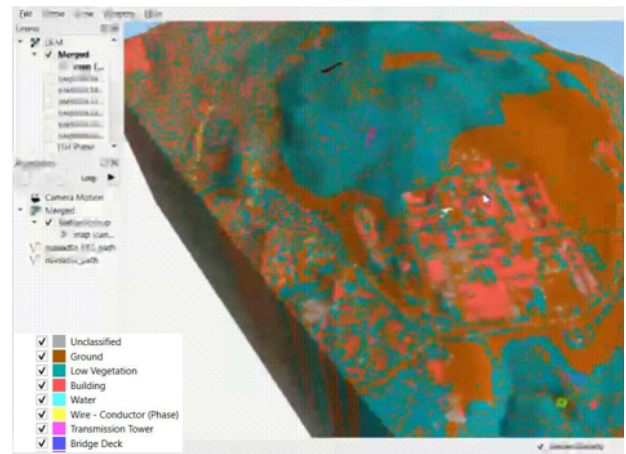


Figure 4. 3D visualization of classified surface data derived from swisstopo laser scanning, enabling distinction between vegetation canopy, buildings, and terrain. The robot trajectory is overlaid for environmental context analysis.

- *Human-in-the-loop* - the beneficiary of robot-based services, e.g., in search and rescue operations, etc.
- *Aim* set depending on whether searching for a person or an object.
- *Authorities* – external party that receives alerts.

In operation, the backend also interfaces with the *Authorities* by transmitting situational alerts and georeferenced event data. This ensures that external decision-makers can respond or authorize actions based on validated GNSS-GIS information. Similarly, the *Operator* and *Human-in-the-loop* interact with the backend through dedicated dashboards or communication channels for configuration, monitoring, and decision support.

Figure 5 illustrates the alert-setup front-end, which provides an operator interface for configuring automated notifications. The *Dashboard* tab aggregates mission statistics and system health metrics, while the *Profile* tab handles user-specific settings to ensure alerts and data streams are tailored to operator roles. The *Alerts* tab allows users to define triggers, such as human detection events, low battery, disturbance, etc. The *Maps (MAP)* tab provides geographic context by overlaying GNSS and GIS layers, enabling operators to visualize event locations in real time. The *Notifications (NOT)* tab manages delivery methods (e.g., email, push, or call) and defines target recipients or user groups for rapid information dissemination. Finally, the *Profile* tab handles user-specific settings, ensuring that alerts and data streams are tailored to mission requirements and operator roles.

The backend of the proposed platform (Fig. 6) is designed to manage data flow, processing, and communication between robots and external services. It enables task scheduling through GIS knowledge inputs, normalizes and streams sensor data, and orchestrates event-driven computations for additional analysis and notifications. Data are securely stored in dedicated databases, while services such as SendGrid provide asynchronous messaging and operator alerts.

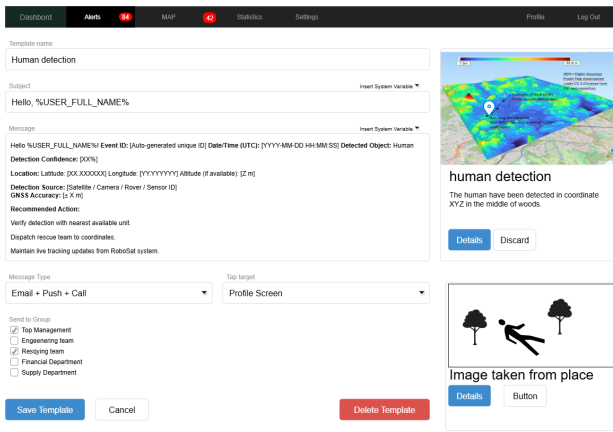


Figure 5. Proposed platform alert-setup front-end

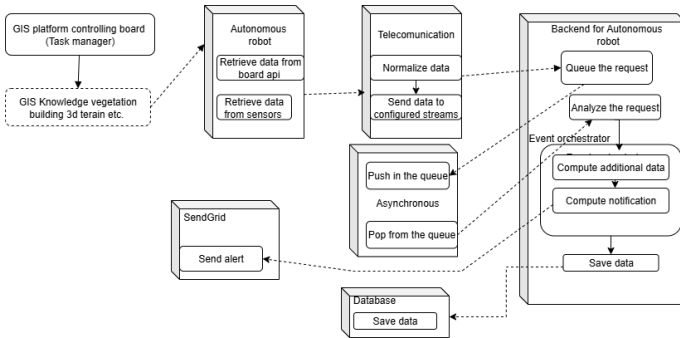


Figure 6. Backend functional architecture of the proposed platform

4. GIS -GNSS integration at various receiver stages

Improving the positioning accuracy of Global Navigation Satellite Systems (GNSS) in signal-degraded environments has long been a challenge for the research community, with non-line-of-sight (NLOS) reception and multipath propagation from surrounding structures being the dominant sources of error in both urban and nature settings. One increasingly studied avenue for addressing these limitations is the fusion of GNSS signal processing with three-dimensional Geographic Information System (GIS) data, an approach that can be applied at two fundamentally different stages of the receiver processing chain: before code correlation takes place, where the receiver still operates on raw in-phase and quadrature (IQ) samples, and after tracking has been completed, where pseudorange and carrier phase observables are already available.

Fig. 7 illustrates the main GNSS receiver stages: pre-correlation, post-correlation, and navigation stages, while Fig. 7 gives details of how one could theoretically integrated GIS data at different stages. For example, at the pre-correlation stage, three-dimensional spatial datasets, including building footprint models, terrain elevation data, and urban structure maps, offer the possibility of conditioning the signal acquisition process using knowledge of the surrounding environment. By applying geometric ray-tracing to predict which satellites are likely to have an unobstructed path to the receiver at a given location, a sky visibility mask can be constructed that constrains the two-dimensional search space of the correlator across both code delay and Doppler shift dimensions. This reduces unnecessary computation on satellites that are pre-

dicted to be blocked and allows signal detection thresholds and integration lengths to be tuned on a per-satellite basis according to the expected received power, rather than applying uniform parameters across the entire constellation. Although prior work has shown that aligning ray-traced path predictions with correlator-level signal samples can meaningfully reduce positioning error in dense built-up areas [1], embedding GIS-derived environmental context directly within the IQ-domain processing pipeline, upstream of any measurement formation, has not been systematically explored and represents the principal novelty targeted by this study.

At the post-correlation stage (see Fig. 7), the three-dimensional building model can transition into a measurement validation and weighting tool that operates on the outputs of the tracking loops. Pseudorange observations whose residuals are inconsistent with the geometric paths predicted by the GIS model can be flagged as likely NLOS-contaminated and excluded from the navigation filter, whether implemented as a weighted least-squares estimator or a particle filter [2]. The shadow matching approach introduced by [3] works by using a 3D city model to predict which satellites should be visible at candidate locations, then comparing these predictions against what the receiver actually observes, with simulation results indicating the method could achieve cross-street accuracy at the meter level, roughly ten times better than standard GNSS positioning in heavily built-up environments. Combining this approach with map-aided pseudorange ranging was subsequently shown by [4] to produce directionally complementary improvements, with each method compensating for the weaknesses of the other depending on street orientation relative to satellite geometry.

As a preliminary validation of post-correlation GIS integration relevant to the present work, a three-dimensional building model of central Tampere was derived from OpenStreetMap data (see an example in Fig. 9) and used to ray-trace and classify GNSS measurements collected via an Android IQ logger. Across 104,743 signal observations, 61.2% were identified as LOS and 38.8% as NLOS; LOS signals exhibited a mean C/N_0 advantage of 6.3 dB over NLOS, with a median building blocking distance of 11.7 m. When the position solution was restricted to LOS-classified measurements only, mean horizontal error decreased by 75.2% under accumulated Doppler ranging, 59.7% with a Kalman filter, and 60.1% using raw pseudoranges, yielding an average improvement of 65% across all three methods. While these preliminary results were obtained in an urban setting using a 3D city model, they nonetheless establish the conceptual and methodological foundation for GIS-based NLOS exclusion and demonstrate that selective use of LOS measurements produces substantial and consistent positioning improvements. The application of equivalent principles to natural environments, where signal obstruction arises not from man-made structures but from terrain morphology, dense vegetation, and mountainous topography, remains largely unexplored in the literature. The present work therefore aims to extend this framework beyond the urban domain, using raw IQ data collected across wilderness test scenarios to develop and validate a GNSS-GIS integration architecture suited to navigation in environments where conventional positioning systems are known to degrade but three-dimensional spatial models derived from terrain and canopy data can be similarly leveraged to characterize and mitigate signal obstruction.

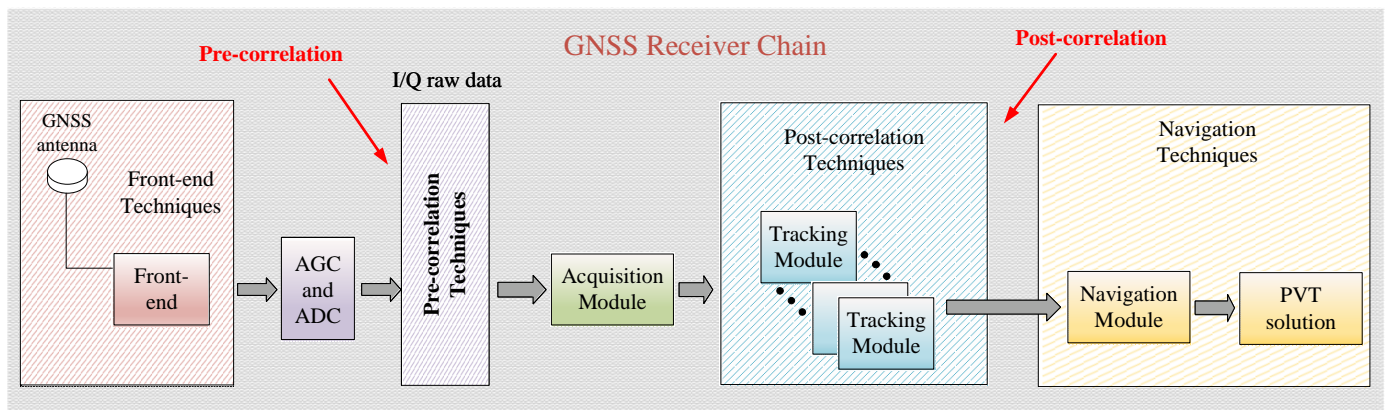


Figure 7. Block diagram illustrating GNSS receiver stages.

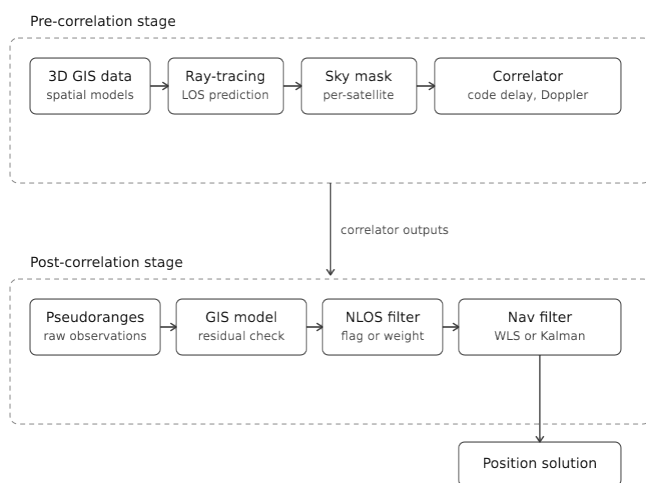


Figure 8. Block diagram illustrating GIS integration ideas at different GNSS receiver stages

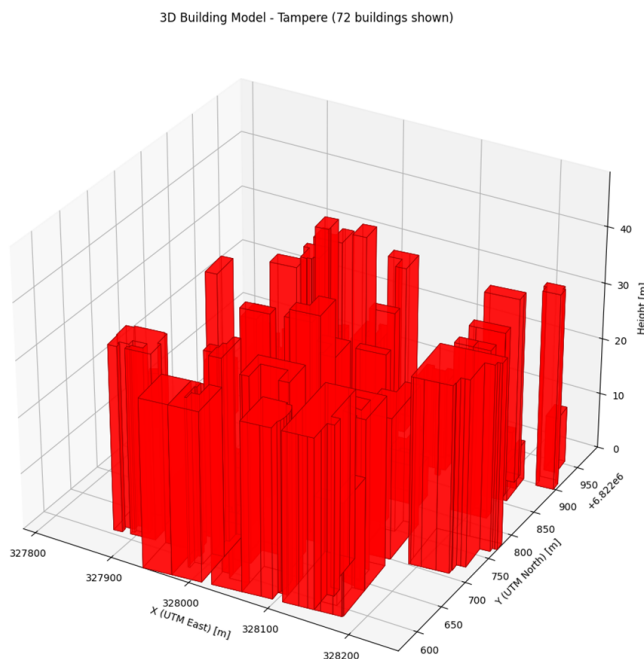


Figure 9. Tampere city 3D model

5. Preliminary results

Multiple trajectory collected with ANYmal robot were analysed to evaluate positioning performance under realistic environmental conditions. These include the real-time navigation solution (RT), the tightly coupled GNSS-INS trajectory (TC), and a post-processed solution (POS) derived from RINEX observations processed using RTKLIB. Ground truth (GT) trajectories were obtained using a prism-based tracking system and were used as a reference for accuracy assessment.

Raw GNSS observations were converted to RINEX format and processed using RTKLIB in post-processing mode. The processing configuration included carrier-phase and pseudo-range measurements, precise ephemerides, and ambiguity resolution. Solutions were initially computed in the global WGS84 reference frame and expressed internally in Earth-Centered Earth-Fixed (ECEF) coordinates. For trajectory comparison and visualization, positions were transformed into a local East-North-Up (ENU) coordinate system using a fixed reference origin. The local ENU frame enables direct interpretation of horizontal errors, drift behaviour, and short-term positioning deviations.

The tightly coupled trajectory was produced by the onboard fusion engine combining GNSS observations and inertial measurements from the integrated IMU. This solution provides improved short-term stability, particularly in areas with degraded satellite visibility. The real-time trajectory represents the standalone navigation output of the receiver and serves as a baseline for comparison with fused and post-processed solutions.

Ground truth positioning was obtained using a Leica MS60 scanning total station tracking a prism mounted on the robotic platform. The system provides millimetre-level positioning accuracy and enables high-frequency measurements suitable for dynamic trajectory evaluation. The prism position was streamed in real time and recorded together with GNSS data, allowing precise temporal synchronization and trajectory comparison. The total station measurements were expressed in the local instrument reference frame and subsequently transformed into the same local ENU coordinate system used for GNSS-derived trajectories. This high-precision ground truth provides a reliable reference for evaluating positioning errors, drift characteristics, and short-term deviations in challenging environments such as forested or partially obstructed areas.

Ground truth trajectories were temporally synchronized and spatially aligned with GNSS-derived trajectories. Time alignment was performed by estimating the optimal time lag and matching epochs using nearest-neighbour association within a defined tolerance window. Spatial alignment was performed using a similarity transformation based on the Umeyama method to estimate translation and rotation between coordinate frames. Robust inlier selection was applied using statistical gating based on median absolute deviation to suppress outliers and intermittent measurement noise.

Environmental context was derived from airborne laser scanning datasets. High-resolution digital elevation models and classified surface representations were used to distinguish terrain, vegetation canopy, and built structures. These layers were co-registered with the trajectories and enable identification of potential signal obstruction zones, multipath-prone areas, and masking angles along the trajectory.

Satellite geometry and measurement conditions were further analysed using skyplot representations derived from RINEX observation files. Skyplots provide satellite elevation and azimuth distributions over time and allow identification of intervals with reduced geometry strength or possible masking effects. When combined with LiDAR-derived environmental layers, this analysis helps associate positioning errors with environmental features.

Figures 10 and 11 illustrate representative trajectory comparisons in the local ENU frame. The TC and POS trajectories closely follow the ground truth, while the real-time solution exhibits larger deviations in segments affected by environmental conditions and terrain variation.

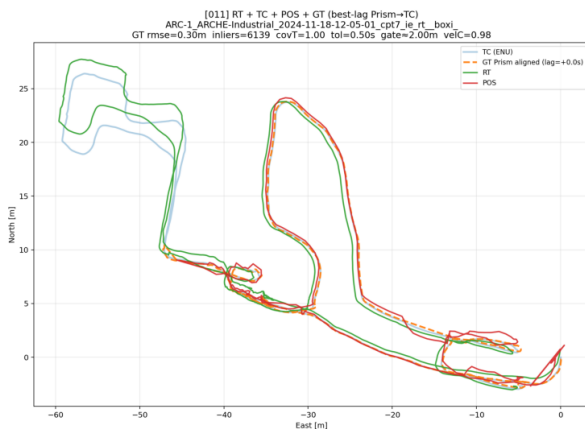


Figure 10. Comparison of real-time (RT), tightly coupled (TC), post-processed (POS), and ground truth (GT) trajectories in the local ENU frame for an industrial test environment. Temporal synchronization and similarity-based spatial alignment were applied prior to comparison.

The objective of this work is to incorporate environmental awareness into GNSS-based navigation by integrating high-resolution geospatial data into the positioning and analysis pipeline. Ongoing work focuses on adapting the observation covariance matrix using environmental indicators derived from GIS layers. Measurement weights can be dynamically adjusted based on satellite elevation, estimated line-of-sight probability, and local surface classification derived from LiDAR. This environment-aware weighting strategy aims to re-

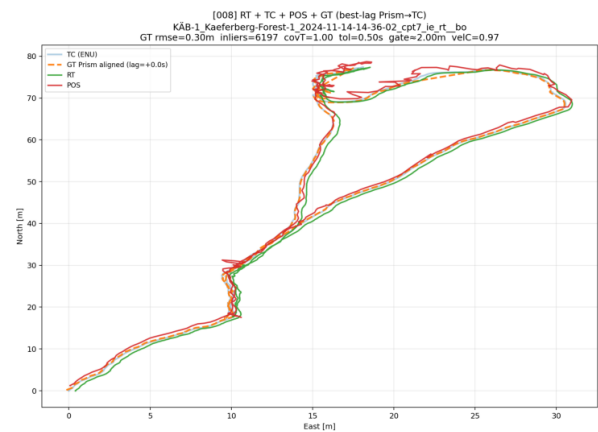


Figure 11. Trajectory comparison in a forested environment illustrating the behaviour of RT, TC, and POS solutions relative to ground truth. Environmental effects such as canopy and terrain variation influence positioning performance.

duce the influence of measurements affected by multipath or partial obstruction and to improve robustness of positioning in complex terrain and urban environments.

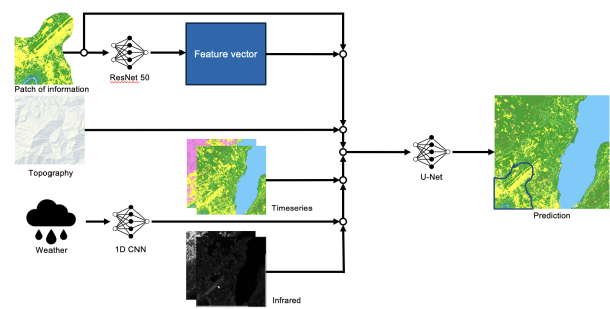


Figure 12. An illustration of the framework we use to predict global terrain changes using local robot observations (presented at the top) aggregated with 3D topographic maps (middle) and past observations from satellites and weather stations (bottom). The target result is a fully inpainted feature map shown on the right.

6. Data alignment

We have used the data from the robot and correlated it with global information from satellites and other sources in two separate experiments on showcasing later possible use for the data.

In the project, the goal was to predict global changes in the terrain using local information gathered by the robot and past global information gathered by a satellite. In addition, we use survey data (provided by the Swiss government) in the form of highly accurate 3D topographic maps. Finally, we also correlate data from weather stations in the area for the past months. Figure 12 illustrates the framework. The ability to use local information to predict global changes is particularly important in applications such as robot navigation. By being able to predict widespread changes in the terrain based on partial observations, the robot can quickly do large-scale adjustments to its path to choose the more energy-efficient or less risky path to traverse wild environments. This is a particularly important

feature in the context of this project where the robot functions as a data collection platform.

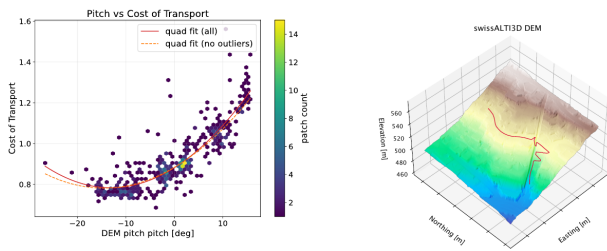


Figure 13. We show that using the collected robot data and aligning it with high-accuracy elevation maps provided by swissALTI3D (from the Swiss government mapping organization), we can predict highly relevant robot centric information. In particular we show that we can predict the Cost of Transport (CoT), i.e. the energy consumption of the robot (left figure) in advance, by looking at the planned trajectory (on the right).

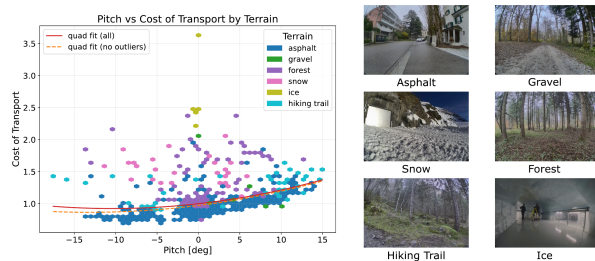


Figure 14. For predicting the Cost of Transport (CoT) across more varying terrain than the solid, even surfaces used in Figure 13, we notice that significantly more data is required. This shows that no correlation is obvious and gives examples of the scene classes.

In a second project, we follow a similar idea, but with a slightly different perspective. We tackle learning the actual cost function for navigation, i.e., how much energy does the robot use to traverse various kinds of terrains, and can we learn to predict this from data? Estimating this Cost of Transport of the robot in advance is a fundamental step towards efficient navigation, data collection, and long-term autonomy. We take previous trajectories and align them on the topographic elevation maps provided by the Swiss government through swissALTI3D. These maps have a resolution of 0.5 m in 2 m × 2 m square grids. The alignment procedure can be seen in Figure 13 on the right. Afterwards we evaluate the cost of transport by taking into account the mechanical and electrical power dissipation happening in the legs during locomotion. This process also requires the use of some heuristics to properly normalize the metric with respect to the tracked robot velocity. Afterwards, we evaluate if using the elevation maps we could have predicted the energy usage as a function of the steepness of the terrain, given an approximate path. We show a high correlation in Figure 13 on the left. This promising preliminary result shows that we can predict one component of energy usage when planning large-scale missions (which is also very relevant for WP5). However, our experiments also show that significantly more data is needed to predict the CoT, for example, on varying terrains as shown in Figure 14 (in our initial evaluations we restricted ourselves to hard/even surfaces).

7. Conclusions

The intermediate results of the ROBOSAT project clearly show that integrating high-resolution GIS data with GNSS observations offers a promising pathway toward improving navigation robustness in wild, unstructured, and environmentally complex areas. By leveraging digital elevation models, vegetation and land-cover layers, and classified surface models derived from laser scanning, the project shows that environmental context can be systematically incorporated into GNSS signal analysis. This context enables more accurate predictions of line-of-sight availability, better characterization of signal obstruction, and improved detection and mitigation of multi-path and NLOS conditions—challenges that traditionally limit GNSS performance in forests, mountainous terrain, or partially obstructed outdoor environments.

Preliminary experiments using the ANYmal robotic platform further validate the potential benefits of GIS-assisted navigation. The comparison between real-time, tightly coupled, and post-processed trajectories against high-precision ground truth reveals that environment-aware modeling can meaningfully enhance positioning reliability. Moreover, the integration of LiDAR-derived terrain information, skyplot-based satellite geometry analysis, and robust data alignment techniques allows the system to link environmental features directly with positioning errors. These insights confirm the relevance of incorporating GIS layers not only for measurement validation and weighting but also for future adaptations of covariance modeling, environment-adaptive filtering, and multi-sensor fusion strategies.

Finally, the deliverable highlights that extending GNSS–GIS integration toward predictive modeling, such as anticipating terrain changes or estimating the robot’s energy consumption (cost of transport), opens new avenues for long-term autonomy and efficient mission planning. Early results show that aligning robot-collected data with high-accuracy elevation maps can already predict meaningful navigation-related quantities, although more diverse datasets are required for broader generalization. Overall, the ongoing work establishes a solid technical foundation for a unified GNSS–GIS processing architecture and sets the stage for the next phases of the project, where quantitative evaluations across wilderness scenarios and multi-sensor datasets will play a key role in achieving reliable, environmentally aware navigation for robotic platforms.

References

- [1] R. Kumar and M. G. Petovello, “3d building model-assisted snapshot positioning algorithm”, *GPS Solutions*, vol. 22, no. 1, p. 12, 2018. DOI: [10.1007/s10291-017-0661-2](https://doi.org/10.1007/s10291-017-0661-2).
- [2] L.-T. Hsu, Y. Gu, and S. Kamijo, “Nlos correction/exclusion for gnss measurement using raim and city building models”, *Sensors*, vol. 15, no. 7, pp. 17 329–17 349, 2015. DOI: [10.3390/s150717329](https://doi.org/10.3390/s150717329).
- [3] P. D. Groves, “Shadow matching: A new gnss positioning technique for urban canyons”, *Journal of Navigation*, vol. 64, no. 3, pp. 417–430, 2011. DOI: [10.1017/S0373463311000087](https://doi.org/10.1017/S0373463311000087).

- [4] M. Adjrad and P. D. Groves, “Intelligent urban positioning: Integration of shadow matching with 3d-mapping-aided gnss ranging”, *Journal of Navigation*, vol. 71, no. 1, pp. 1–20, 2018. DOI: [10.1017/S0373463317000509](https://doi.org/10.1017/S0373463317000509).